Selective Mode Excitation and Detection of Micromachined Resonators

Albert Prak, Miko Elwenspoek, and Jan H. J. Fluitman, *Member, IEEE*

***Abstract*—Distributed mechanical systems such as micromachined resonant strain gages possess an infinite number of modes of vibration. Mostly, one is interested in only one or a few modes. A method is described with which only the desired modes are excited and detected. This is achieved by geometrically shaping the elements used for excitation and detection of the vibration. The method is based on the orthogonality principle, which is valid for a variety of structures and vibrations. In this paper we have restricted ourselves mainly to transversal vibrations of prismatic beams, clamped on both sides (microbridges). The design rules for obtaining the shapes for most commonly used excitation and detection mechanisms are deduced and the effect of axial stress on the suppression of unwanted modes is discussed. The theory was verified by experiments on resonators with selective mode excitation using different excitation mechanisms, as well as on resonators with both selective excitation and detection.**

I. Introduction

MICROMECHANICAL resonator sensors [1], [2] are in an increasing field of interest because of their great sensitivity and quasi-digital output. Due to their distributed mechanical character, these systems generally have an infinite number of modes of vibration. By the analytical method of modal analysis [3], it can be made clear that the modes, which are required to describe the vibration, are closely related to the spatial dependence of the excitation load. Most excitation methods utilize on-chip electrodes. By shaping these electrodes, the excitation load can be controlled, giving us control over which modes are excited and how strong. The modes that will be detected depend also strongly on the shape of the detection elements. When no special attention is paid to the design of excitation and detection elements, multiple modes will be excited and detected. However, resonant sensors are usually operated at one eigenfrequency (usually the first). The appearance of other modes can lead to degrading sensor performance. For example, when the resonator is supplied with an electronic circuitry (to provide an oscillator), the oscillator can lock in on the wrong mode. By using selective mode excitation and selective mode detection, the condition for oscillation is met for an unambiguous frequency over a wide range. This increases the measurement range of the resonant strain gage. Another advantage is that less energy will be coupled in unwanted modes, resulting in improved sensor performance. Possible disadvantages are that a more complex mask design is required and that the electrode geometry for suppression of unwanted modes also decreases the efficiency of the desired modes somewhat (typically 25%).

Manuscript received April 23, 1992; revised November 11, 1992. Subject Editor, R. O. Warrington.

The authors are with the MESA Research Institute, University of Twente, 7500 AE Enschede, the Netherlands.

IEEE Log Number 9206695.

II. Theory of Selective Mode Excitation

Small transversal movements of a viscously damped prismatic beam subject to an axial force, N, and a driving load, $P(x, t)$ (see Fig. 1), are described by the following linear, inhomogeneous differential equation [4]:

$$\hat{E}Iv''''(x, t) - Nv''(x, t) + \rho A\ddot{v}(x, t) + c\dot{v}(x, t) = P(x, t), \quad (1)$$

with $v(x, t)$ the deflection, I the moment of inertia, c the viscous drag parameter (force per unit length per unit velocity), and A the cross-sectional area of the beam ($A = bh_b$, with b the width and h_b the thickness). For beams with $b >> h_b$, $\hat{E} = E/(1 - \nu^2)$ holds, with E Young's modulus and ν Poisson's ratio of the beam material, ρ is the density of the beam material. A prime and a dot denote differentiation with respect to x and t, respectively. We assume that separation of space and time coordinates is possible and that the time-dependent parts of v and P are harmonic functions:

$$v(x, t) = \bar{v}(x)e^{j\omega t} \qquad P(x, t) = \bar{P}(x)e^{j\omega t}. \quad (2)$$

Throughout this paper, an overbar will generally represent the (complex) amplitude of a harmonic quantity. The beam can be excited with moments and forces which both can be concentrated or distributed. In this paper, only distributed moments (m) and distributed forces (D) will be considered:

$$\bar{P}(x) = \bar{D}(x) - \bar{m}'(x). \quad (3)$$

It can be shown that, if homogeneous boundary conditions are taken into account, the solution of (1) can be written as the following expansion series [3]:

$$\bar{v}(x) = \sum_{r=1}^{\infty} \bar{y}_r v_r(x). \quad (4)$$

In this equation, $v_r(x)$ are the solutions of the homogeneous equation of the undamped system:

$$\hat{E}Iv''''(x) - Nv''(x) - \rho A\omega^2 v(x) = 0. \quad (5)$$

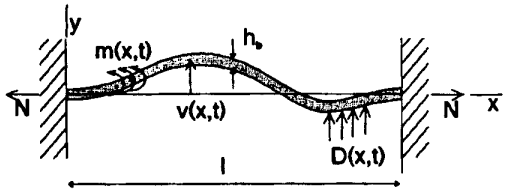

Fig. 1. Cross section of the structure under consideration.

The functions $v_r(x)$ are the mode shapes. The mode shapes and corresponding eigenfrequencies, ω_r, can be calculated using standard mechanics. Solutions are given in [2]. In (4) y_r are the generalized (normal) coordinates. They indicate how strong a mode is represented in the vibration. A very important property of the mode shapes is that they are orthogonal [3]:

$$\frac{1}{l}\int_0^l v_r(x)\,v_s(x)\,dx = \delta_{r,s}. \tag{6}$$

In this equation, l is the length of the beam and $\delta_{r,s}$ the Kronecker delta. It is this orthogonality principle which is the key to selective mode excitation and detection.

Besides the orthogonality, (6) also defines the normalization of the modes. By substituting (4) into (1), using the fact that $v_r(x)$ satisfies (5), multiplying by $v_s(x)$, integrating over the beam length l and applying (6), we finally find

$$M_r\ddot{\bar{y}}_r + F_r\dot{\bar{y}}_r + K_r\bar{y}_r = \bar{P}_r, \qquad r = 1, 2, \cdots. \tag{7}$$

M_r, F_r, and K_r denote the modal mass, modal damping constant, and modal stiffness respectively. Taking the normalization of (6) into account, we find the following relations for these modal constants:

$$M_r = \rho A l \qquad F_r = cl \qquad K_r = \rho A l \omega_r^2. \tag{8}$$

In (7), $\bar{P}_r$ are the modal (generalized) loads. They are a measure of the efficiency with which a specific mode is excited. They are the expansion coefficients of the total load:

$$\bar{P}_r = \int_0^l \bar{P}(x)\,v_r(x)\,dx \tag{9a}$$

$$\bar{P}(x) = \frac{1}{l}\sum_{r=1}^{\infty} \bar{P}_r v_r(x). \tag{9b}$$

From (7) it is seen that the system can be described as an infinite number of independent lumped elements (modes), every element being driven by its own generalized load.

For applications in resonant strain gages, one is interested in a limited number of modes (mostly the first one only). For optimum sensor performance, all other modes should be suppressed. It is seen from (7) that only modes for which $\bar{P}_r \neq 0$ will be excited. By comparing (9a) to the orthogonality relation (6), we immediately see that this can be achieved by choosing $\bar{P}(x)$ proportional to the shapes of the modes to be excited.

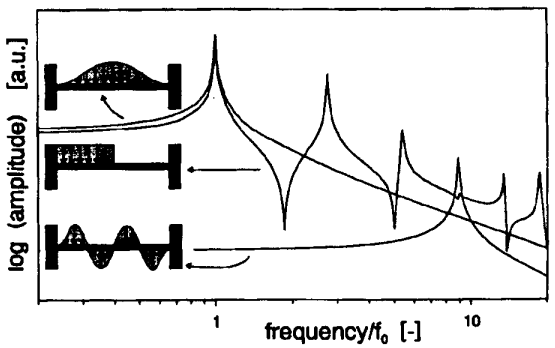

Fig. 2. Computed amplitude Bode plots of a microbridge excited with a rectangular load and loads for excitation of modes 1 and 4 only. The displacement was computed at 25% of the beam length from the beam edge.

In many cases, the excitation load is applied by means of excitation mechanisms utilizing on-chip electrodes. By geometrically shaping these electrodes, we have refined control over the spatial dependence of the excitation load, and thus over the modes being excited.

Some example amplitude Bode plots of the very important case where only a single mode is excited are given in Fig. 2. The spectrum of an rectangular excitation element which excites multiple modes is also shown.

III. Design Rules for Excitation Mechanisms

Micromechanical resonators can be excited by a number of mechanisms. From a mechanical point of view, the mechanisms can be divided into two categories, namely mechanisms which generate forces and mechanisms which generate moments. We will now derive the design rules for the shapes of the excitation elements of commonly used excitation mechanisms. In doing so, we use simple, linearized models for the mechanisms.

A. Electrostatic Excitation

Electrostatic excitation (see e.g. [5] and [6]) is probably the force mechanism that is used most often. The Coulomb force between two parallel plates, one of which is placed on the resonator, is used to exert a transversal distributed force, $\bar{D}(x)$, on the resonator. When side effects of the electrostatic field between the plates are neglected and the deflections (both static and dynamic) are assumed to be small with respect to the gap spacing, we find the following expression for the harmonic component of the load:

$$\bar{P}(x) = \bar{D}(x) = \frac{\epsilon_0}{d^2} U_{dc}\bar{U}_{ac} w(x), \tag{10}$$

with $w(x)$ the width of the electrode and ϵ_0 the permittivity of free space. The parameter d is the spacing between the electrodes, and U_{dc} and U_{ac} are the dc and ac voltages across the electrodes, respectively. The biasing dc voltage is required to get a component with the frequency of the ac voltage. By combining (9b) and (10), the design

rule for the shape of the electrode is obtained:

$$w(x) = \frac{d^2}{l\epsilon_0 U_{dc} U_{ac}} \sum_{r=1}^{\infty} \bar{P}_r v_r(x). \quad (11)$$

In this equation, $\bar{P}_r$ are the *desired* generalized loads, and $v_r(x)$ the corresponding mode shapes. If, for example, only the first mode has to be excited, all desired generalized loads, except $\bar{P}_1$, are zero. From (11) it is seen that the electrode shape should be chosen proportional to the first mode shape. Note that this shape does not excite the first mode with maximum efficiency (which is obtained if the electrode covers the entire beam). The efficiency is decreased by 24.2% by using the mode 1 selective pattern (computation for a microbridge without axial strain).

For excitation of the second or higher modes, the required load, and thus the width, appear to be negative in one or more areas. In practice, this can be achieved by reversing either the ac or dc voltage in the areas where $w(x) < 0$ and making the actual width equal to $|w(x)|$.

When the static deflection caused by the bias voltage cannot be neglected, the excitation force is no longer proportional to the electrode width. The force increases in the regions where the static deflection is large, thereby disturbing the sophisticated force distribution. In that case, the electrode shape must be redesigned.

B. Piezoelectric and Dielectric Excitation

Piezoelectric excitation [7], [8] is a typical moment mechanism. The mechanism is based on the fact that the length of a thin layer on top of the beam is periodically changed (bimorph excitation). The film consists of a piezoelectric material (e.g. ZnO) sandwiched between two electrodes. A voltage across the electrodes results in a bending moment. This moment is given by

$$\bar{m}(x) = \frac{d_{31} \bar{U}_{ac} E_f h_b}{2} w'(x), \quad (12)$$

where d_{31} is the piezoelectric constant relating the field strength in the y direction to the strain in the x direction, $\bar{U}_{ac}$ the voltage across the film, E_f Young's modulus of the film material, and $w(x)$ the width of the film. In (12), the film was assumed to be much thinner than the beam. Combining (3), (9b), and (12) yields the design rule for piezoelectric excitation:

$$w(x) = -\frac{2}{d_{31} \bar{U}_{ac} E_f h_b l} \sum_{r=1}^{\infty} \bar{P}_r \iint v_r(x)\, dx\, dx. \quad (13)$$

Here $\bar{P}_r$ are again the desired loads. So the width of the piezoelectric layer (or the width of the electrode covering it) should be chosen proportional to the twice integrated shapes of the modes to be excited. Two integration constants will occur. In the case of a microbridge, the integration constants can be chosen arbitrarily (any function of the form $w(x) = c_1 x + c_2$ can be added to the electrode shape). This gives us the possibility to design the width such that it is positive along the entire beam. This avoids the need to reverse the voltage in one or more regions. For cantilever beams, clamped at $x = 0$ and free at $x = l$, the integration constants should be chosen such that $w(l) = 0$ and $w'(l) = 0$ (i.e., $c_2 = c_1 = 0$). Otherwise, a concentrated force and moment will be introduced at the beam tip, resulting in excitation of multiple modes.

The elongation of the top film can also be accomplished by using a dielectric film instead of a piezoelectric film. A voltage across the electrodes will squeeze the dielectric film somewhat. As a result, the film will undergo an elongation. This mechanism has been demonstrated in [9]. Apart from a proportionality constant, the geometrical dependence of the induced moment, and consequently the design rule for the electrode shape, are the same as for piezoelectric excitation.

C. Thermal Excitation

Another way to elongate the top film of the beam is by thermal heating [10], [11]. This can be done either by dissipating electrical or optical energy. If the thermal diffusion constant and (in the case of optothermal excitation) the penetration depth of the incident light are small compared with the beam thickness, the mechanical moment is given by [11]

$$\bar{m}(x) = \frac{E h_b^3 \alpha}{24k} \bar{W}'(x), \quad (14)$$

where α is the coefficient of thermal expansion, k the thermal conductivity of the beam material, and $\bar{W}(x)$ the dissipated thermal power per unit length. When the conditions mentioned above are no longer met, the proportionality constant in (14) will become complex. However, the moment will remain proportional to $\bar{W}'(x)$.

In the case of optothermal excitation, the beam can be placed in a light spot of homogeneous intensity. Selective mode excitation can be obtained by depositing a film with variable width and an absorption coefficient different from the beam material. For the dissipated heat per unit length, we find $\bar{W}(x) = \bar{I}_0[w(x)(a_f - a_b) + ba_b]$, where $\bar{I}_0$ is the intensity of the light, a_b and a_f the absorption coefficients of beam and film respectively, and $w(x)$ the width of the film. The design rule for the shape of the film is again an equation like (13), with a different factor in front of the sum sign. Note that the absorption coefficient of the area beside the film need not be zero; it can be accounted for in one of the integration constants (see the design considerations above in subsection B).

When using electrothermal excitation, the heat is produced by a current through a resistive layer on top of the beam. For the resistance per unit length of a homogeneous film with constant thickness $R(x) = \rho_f / h_f w(x)$ holds, with ρ_f, h_f, and w the resistivity, the thickness, and the width of the resistive film, respectively. For the harmonic component of the dissipated power per unit length we find $\bar{W}(x) = i_{dc} \bar{i}_{ac} R(x)$, where i_{dc} and i_{ac} are the dc and ac currents through the resistive layer respectively.

Combining the results obtained so far, we find

$$\bar{m}(x) = \frac{Eh_b^3\alpha}{24k}\frac{i_{dc}\bar{i}_{ac}\rho_f}{h_f}\left(\frac{1}{w(x)}\right)'. \quad (15)$$

One finally finds the following condition for the film width:

$$w(x) = -\frac{Eh_b^3\alpha}{24k}\frac{i_{dc}\bar{i}_{ac}\rho_f l}{h_f}\frac{1}{\sum_{r=1}^{\infty}\bar{P}_r\iint v_r(x)\,dx\,dx}, \quad (16)$$

where $\bar{P}_r$ are the desired modal loads, and $v_r(x)$ the corresponding mode shapes. The final shape is the reciprocal of the shape found for the standard bimorph excitation.

IV. Design Rules for Detection Mechanisms

A. Capacitive Detection [6], [12]

The configuration used for electrostatic excitation can be applied for detecting the vibrations by measuring the currents as a result of the capacitor changes caused by the vibration. When the amplitude of vibration and the static deflection (caused by the required biasing voltage) are negligible with respect to the gap distance, the following expression holds for the detection current:

$$\bar{i} = \frac{U_{dc}\epsilon_0}{d^2}\int_0^l w(x)\bar{v}(x)\,dx = \frac{U_{dc}\epsilon_0}{d^2}\,l\sum_{r=1}^{\infty}\bar{y}_r w_r. \quad (17)$$

In the last step, both $w(x)$ and $v(x)$ were expanded in the mode shapes and the orthogonality relation (6) was applied. For $v(x)$, this expansion is shown in (4). The expansion of the electrode width is

$$w_r = \frac{1}{l}\int_0^l w(x)\,v_r(x)\,dx \quad (18a)$$

$$w(x) = \sum_{r=1}^{\infty} w_r v_r(x). \quad (18b)$$

From (17), it is immediately seen that only modes for which $w_r \neq 0$ will be detected. In other words, to detect a specific mode (or combination of modes), the electrode should be shaped proportional to the sum of the shapes of the modes to be detected. This design rule is the same as we have found for electrostatic excitation. This similarity can be traced to the reciprocity of both mechanisms.

B. Piezoelectric Detection

Since piezoelectricity is a reversible effect, a piezoelectric layer can also be used for detection of vibrations. Either a voltage or a current can be measured. We will discuss here the case where the detection element is short-circuited. Apart from a proportionality constant, the design rule will be the same for other load impedances. Equation (19) holds for the current generated by the beam vibrations [12]:

$$\bar{i} = -d_{31}\hat{E}\frac{h_b}{2}\int_0^l w(x)\bar{v}''(x)\,dx = -d_{31}\hat{E}\frac{h_b}{2}\sum_{r=1}^{\infty}\tilde{w}_r\bar{y}_r. \quad (19)$$

In the last step of (19), $w(x)$ and $\bar{v}''(x)$ were expanded in the second derivatives of the mode shapes, after which an orthogonality relation for the second derivatives was used. The expansion of $\bar{v}''(x)$ follows directly from (4), while the expansion of $w(x)$ we used reads

$$\tilde{w}_r = \int_0^l w(x)\,v_r''(x)\,dx \quad (20a)$$

$$w(x) = \sum_{r=1}^{\infty}\frac{\hat{E}I}{\rho A l\omega_r^2}\tilde{w}_r v_r''(x). \quad (20b)$$

The orthogonality relation for the second derivatives can be found from (5) and (6) and reads

$$\frac{\hat{E}I}{\rho A l\omega_r^2}\int_0^l v_r''(x)\,v_s''(x)\,dx = \delta_{r,s}. \quad (21)$$

This equation holds only for axially unloaded beams ($N = 0$).

From (19), it is seen that only modes for which $\tilde{w}_r \neq 0$ contribute to the current. So the electrode width should be chosen proportional to $v_r''(x)$ of the desired modes. For selective piezoelectric *excitation* we found that the width should be chosen proportional to the two times integrated mode shapes. Since the mode shapes are exclusively composed of the trigonometric functions *sin*, *cos*, *sinh*, and *cosh*, the conditions for the electrode width of structures with piezoelectric detection are the same. The only difference is that, for piezoelectric detection, the design rule holds for axially unloaded beams only and there are no integration constants which we can use for optimizing the shape. Again, the similarity is based on the reciprocity of the mechanisms.

In most cases, $w(x)$ will change sign along the x axis. However, in the case of microbridges, a constant may be added to $w(x)$ such that the width is positive along the entire beam. The added constant detects the difference in angular rotation at $x = 0$ and $x = l$, which is obviously zero for every mode of an ideal microbridge.

C. Piezoresistive Detection

Vibrations can be detected selectively by piezoresistive strain gages on top of the vibrating structure. To derive the design rule, it is assumed that the gage factor of the piezoresistive material $G >> 1$, so the change in the resistance of the resistive pattern is determined by the change in resistivity of the piezoresistive material and not by the dimensional change of the strain gage. This assumption certainly holds for silicon and poly-silicon strain gages [13]. For changes in the resistance (which can be regarded as the output signal) the following relation

holds ($h_b >> h_f$, h_f being the film thickness):

$$\bar{R} = \int_0^l \frac{\bar{\rho}_f}{h_f w(x)}\,dx = G\rho_0 \frac{h_b}{2h_f}\int_0^l \frac{\bar{v}''(x)}{w(x)}\,dx, \quad (22)$$

with ρ_f the actual resistivity and ρ_0 the resistivity at zero applied strain. By expanding $w(x)$ according to

$$\tilde{w}_r = \int_0^l \frac{v_r''(x)}{w(x)}\,dx \quad (23a)$$

$$w(x) = \frac{1}{\sum_{r=1}^{\infty} \frac{\hat{E}I}{\rho A l \omega_r^2}\tilde{w}_r v_r''(x)}, \quad (23b)$$

a design rule very much like (19) is obtained:

$$\bar{R} = G\rho_0 \frac{h_b}{2h_f}\sum_{r=1}^{\infty} \bar{y}_r \tilde{w}_r. \quad (24)$$

A mode can be detected only if its expansion coefficient $\tilde{w}_r \neq 0$. From (23b) it is seen that the shape should be chosen proportional to the reciprocal of the sum of the second derivatives of the modes to be detected. The shapes resemble the shapes found for electrothermal excitation, although the mechanism is based on another physical effect. Just as in the piezoelectric case, the design rule holds only for axially unloaded beams. At the points of inflection of a mode shape, $v_r''(x)$ is zero; consequently the electrode width will be infinite. Since this cannot be realized, small contributions of unwanted modes will always be present in the output signal.

V. Effect of Axial Stress

The principle of resonant sensors is that the resonance frequency is modulated by the measurand. This modulation can be achieved by changing either the mass or the stiffness of the resonator [6]. In both cases, the eigenfrequencies of the resonator are affected. The mode shapes are only sensitive to stiffness modulation. They depend on the axial stress σ ($\sigma = N/A$); thus $v_r = v_r(x, \sigma)$. However, the electrode shape, which is derived from the mode shapes, will not change as the stiffness changes. Therefore, the selective mode excitation and detection elements will generally be designed for a specific set point of the axial load. The effect of an axial load on the excitation efficiencies (i.e., the generalized loads) will now be derived.

Suppose that an excitation element has been designed such that at $\sigma = \sigma_0$ the generalized loads are $\bar{P}_r(\sigma_0)$. For the generalized load, the following relation as a function of the stress σ holds (substitution of (9b) at σ_0 into (9a) at σ):

$$\bar{P}_s(\sigma) = \sum_{r=1}^{\infty} \bar{P}_r(\sigma_0) H_{r,s}(\sigma, \sigma_0), \quad (25)$$

with

$$H_{r,s}(\sigma, \sigma_0) = \frac{1}{l}\int_0^l v_s(x, \sigma) v_r(x, \sigma_0)\,dx. \quad (26)$$

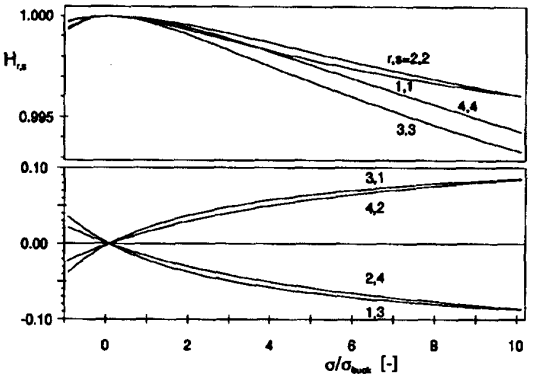

Fig. 3. $H_{r,s}$ as a function of the normalized axial stress for $\sigma_0 = 0$ and r, $s \leq 4$. When r and s have different parities, $H_{r,s}$ equals zero.

$H_{r,s}$ is a good measure of the sensitivity of selective mode excitation to axial stress. We have evaluated $H_{r,s}(\sigma, \sigma_0)$ for $\sigma_0 = 0$ for all r, $s \leq 4$. The results are shown in Fig. 3. Note that $H_{r,s}$ equals the Kronecker delta when $\sigma = \sigma_0$. In the special case where only one mode (say mode r) is excited at σ_0, $H_{r,s}$ represents the generalized load of mode s at an axial stress σ relative to the generalized load of mode r at a stress σ_0. In Fig. 3, the axial stress is normalized with respect to the absolute value of the buckling stress, for which $\sigma_{buck} \sim 3.39\hat{E}h_b^2/l^2$ holds [2]. The decrease of $H_{s,s}$ caused by an axial stress is of no importance over the entire stress range. When $r \neq s$, and r, s have different parities, mode r remains suppressed for all stresses. This is a result of the fact that symmetrical and antisymmetrical modes alternate. However, when r and s have the same parity, the cross effect to other modes is typically a few percent at the buckling stress.

Additional study reveals that for the detection mechanisms, the effect of an axial stress is also described by the function $H_{r,s}$. However in the piezoelectric and the piezoresistive case the reference stress σ_0 should equal zero. Further, the output signals of the detection mechanisms are proportional to the amplitudes of the modal coordinates. The effect of an axial force on these modal coordinates is in turn also described by the function $H_{r,s}$ (see (7) and (25)). This means that in resonators in which both excitation and detection elements are shaped according to the design rules, unwanted modes are suppressed by an amount $H_{r,s}^2$, instead of $H_{r,s}$. As was shown previously, the shapes for technologically compatible excitation and detection mechanisms turn out to be equal, so the use of one-port resonators [12], [14] is very favorable from the point of view of selective mode excitation/detection.

VI. Experiments

Test structures have been realized for excitation with a force and a moment (electrostatic and dielectric excitation respectively). Details of the structures are given in Fig. 4. A photograph of the dielectrically excited structures is presented in Fig. 5. Since both excitation mechanisms are

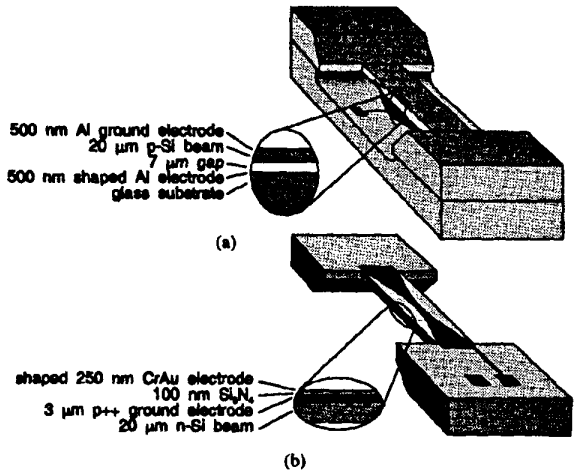

Fig. 4. Test structures with (a) electrostatic and (b) dielectric excitation. The beams are 5 mm long and 1 mm wide.

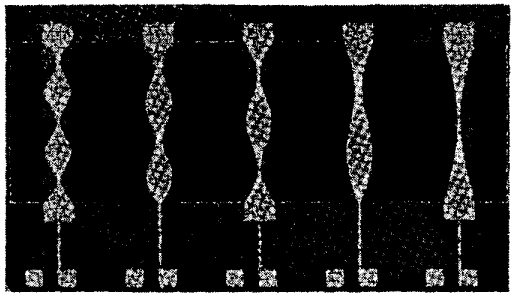

Fig. 5. Photograph of the test structures with dielectric excitation for excitation of modes 1 (right) to 5 (left). The electrode shapes are proportional to the two times integrated mode shapes.

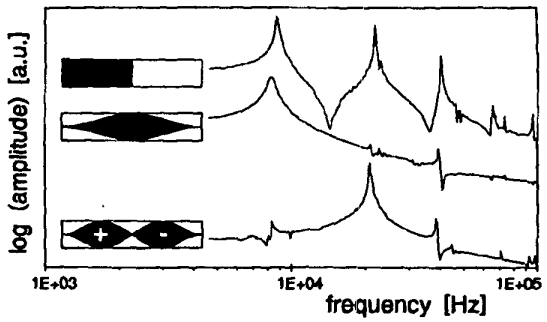

Fig. 6. Amplitude of Bode plots of the electrostatically excited test samples. From top to bottom: excitation of multiple modes and selective excitation of mode 1 and 2, respectively. The electrode shapes are sketched next to the curves. The vibrations were detected interferometrically at 25% of the beam length from the edge. Note the resemblance with the theoretical curves in Fig. 2.

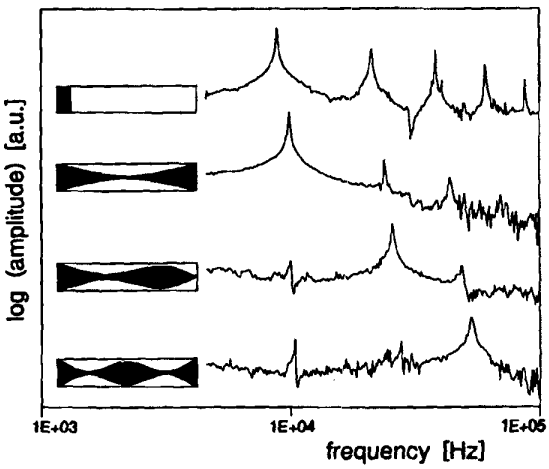

Fig. 7. Amplitude Bode plots of the test samples with dielectric excitation. From top to bottom: excitation of multiple modes and selective excitation of modes 1, 2, and 3, respectively. The locations of detection were at 10, 50, 25, and 25% of the beam length from the edge, respectively.

quadratic effects, the applied voltages have been biased with a dc voltage of typically 10 V. The ac driving voltage was 1 V rms. The motion was detected nonselectively by means of a Michelson interferometer.

The results of the electrostatically excited structures are shown in Fig. 6. The ac voltages of the two halves of the electrode for excitation of the second mode were in antiphase. The results of the dielectrically driven structures are shown in Fig. 7. The first three resonance frequencies of the test samples are approximately 8, 20, and 40 kHz. Due to mutual thickness differences of the beams, these frequencies vary slightly from beam to beam.

In all cases, the suppression of unwanted modes is clear. Mode 2 of the electrostatic device (Fig. 6) is suppressed by approximately 30 dB when using the mode 1 selective pattern. Mode 1 is suppressed 40 dB by the mode 2 selective pattern. Similar suppression ratios are obtained for the dielectrically excited samples. The weak presence of unwanted modes is ascribed to the fact that the shaped electrode did not exactly match the shapes obtained by the design rules (the electrodes were composed of a limited number of rectangles), and to the fact that the beams did not have exactly the same length as the electrodes (due to underetching). Further, the electrode shapes were designed for axially unloaded beams. However, due to the fabrication process, some stress is present in the beams. The appearance of unwanted modes can also be attributed to the inhomogeneity of the beam thickness. For the electrostatic structure, a slight misalignment of the shaped electrode with respect to the beam can also have some effect.

Finally, we have performed measurements on electrostatic devices in a one-port configuration, i.e., with both selective excitation and detection. A quadratic suppression of unwanted modes is expected from the theory. The measurements were performed on the first three modes of a nonselective structure with an electrode covering one half of the beam (sample I), and a structure with an electrode selective to mode 1, however with a beam-to-electrode misalignment of approximately 100 μm (sample II).

The results are summarized in Table I. The polar ad-

TABLE I
RESULTS OF ONE-PORT ADMITTANCE MEASUREMENTS

Sample	Mode	U_{dc} [V]	Q_r [−]	f_{res} [Hz]	$\varnothing_{loop}$ [nA/V]	$w_{r,exp}$ [mm]	$w_{r,theor}$ [mm]
I	1	40.0	500	8460	67	0.42	0.42
I	2	40.0	280	21180	18	0.46	0.43
I	3	40.0	1220	39170	7	0.19	0.18
II	1	30.0	1510	8486	213	0.58	0.63
II	2	40.0	2090	20430	1.5	0.05	0.04

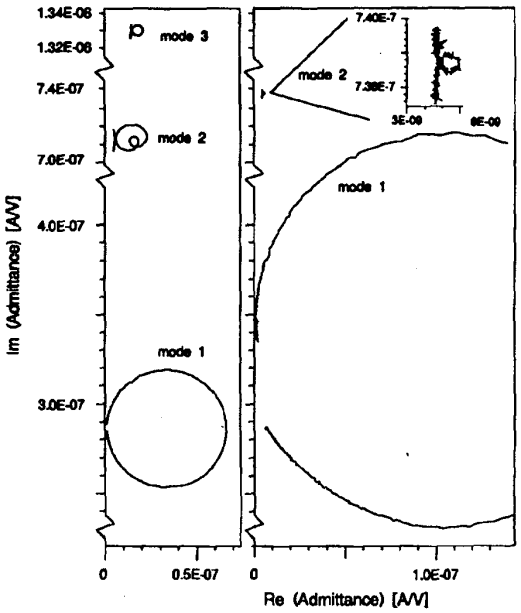

Fig. 8. Polar admittance plots of the one-port measurements on a nonselective resonator (left) and of a resonator which is selective to mode 1 (right), the latter having a beam-to-electrode misalignment of approximately 100 μm.

mittance plots are shown in Fig. 8. For quantitative interpretation of the results, we have derived an expression for the diameter of a resonance loop: $\varnothing_{loop} = U_{dc}^2 \epsilon_0^2 w_r^2 l^2 Q_r / (M_r \omega_r d^4)$, with U_{dc} the bias voltage, Q_r the modal quality factor, which can be found experimentally from the $\pm 45°$ points, M_r the modal mass (0.28 mg) given by (8), ω_r the modal angular resonance frequency, d the gap spacing (23 μm), l the length of the beam (5 mm), and w_r the expansion coefficient of the electrode width. The w_r's can be found either experimentally (from the loop diameter) or theoretically by (18). Both values are listed in Table I. It can be concluded that good agreement exists between the experimental and theoretical values of w_r. Further it is seen that in spite of its relatively high Q, a reduction of w_r by only a factor 10 makes the mode hardly detectable. This is a consequence of the quadratic suppression. The contribution of the mode is thus reduced by a factor 100. The effectiveness of the selective mode principle is further stressed by the fact that modes 3 and higher of sample II, as well as modes 2 and higher of a sample with a much better beam-to-electrode alignment were below the detection limit of our measurement equipment.

VII. CONCLUSIONS

To improve the performance of resonant strain gages, only the relevant modes should be excited and detected. This can be achieved by shaping the electrodes utilized in the excitation and detection mechanisms. A theory and design rules are given with which the shapes of the electrodes of commonly used excitation and detection mechanisms can be designed such that only the desired modes of vibration are excited and detected. We found the same design rules for technologically compatible excitation/detection pairs. This makes the use of one-port resonators very attractive. Experiments on single-mode excitation of test structures with various excitation mechanisms have been performed, and show a clear reduction of unwanted modes. Experiments on electrostatic structures demonstrate that an even better reduction is obtained by operating the resonator in a one-port configuration. Contributions of unwanted modes of well-aligned structures were below the detection limit of the experimental equipment.

ACKNOWLEDGMENT

The authors would like to thank H. Tilmans for fruitful discussions and R. Legtenberg for his help in preparing the samples.

REFERENCES

[1] G. Stemme, "Resonant silicon sensors," *J. Micromechanics and Microengineering*, vol. 1, pp. 113–125, 1991.
[2] H. A. C. Tilmans, M. Elwenspoek, and J. H. J. Fluitman, "Micro resonant force gauges," *Sensors and Actuators A*, vol. 30, nos. 1-2, pp. 35–53, 1992.
[3] L. Meirovitz, *Analytical Methods in Vibrations*. London: Collier-Macmillan, 1967.
[4] S. P. Timoshenko, D. H. Young and W. Weaver, *Vibration Problems in Engineering*, 4th ed. New York: Wiley, 1974, ch. 5.
[5] C. Linder, E. Zimmerman, and N. F. de Rooij, "Capacitive polysilicon resonator with MOS detection circuit," *Sensors and Actuators A*, vols. 25-27, pp. 591–595, 1991.
[6] R. T. Howe, "Resonant microsensors," in *Proc. 4th Int. Conf. Solid State Sensors and Actuators (Transducers '87)* (Tokyo, Japan), June 2–5, 1987, pp. 843–848.
[7] J. G. Smits *et al.*, "Resonant diaphragm measurement system with ZnO on Si excitation," *Sensors and Actuators*, vol. 4, p. 565–571, 1983.
[8] C. J. van Mullem, F. R. Blom, J. H. J. Fluitman, and M. Elwenspoek, "Piezoelectrically driven silicon beam force sensor," *Sensors and Actuators A*, vols. 25-27, pp. 379–383, 1991.
[9] S. Bouwstra *et al.*, "Excitation and detection of micromechanical structures using a dielectric thin film," *Sensors and Actuators*, vol. 17, pp. 219–223, 1989.
[10] T. S. J. Lammerink, M. Elwenspoek, and J. H. J. Fruitman, "Frequency dependence of thermal excitation of micromechanical resonators," *Sensors and Actuators A*, vols. 25-27, pp. 685–686, 1991.
[11] T. S. J. Lammerink, M. Elwenspoek, and J. H. J. Fluitman, "Optical excitation of micromechanical resonators," in *Proc. Micro Electro Mechanical Systems (MEMS '91)* (Nara, Japan), Jan. 31–Feb. 2, 1991, pp. 160–165.
[12] H. A. C. Tilmans, D. J. Yntema, and J. H. J. Fluitman, "Single element excitation and detection of (micro-) mechanical resonators,"

in *Proc. 6th Int. Conf. Solid State Sensors and Actuators (Transducers '91)* (San Francisco), June 24-27, 1991, pp. 533-537.
[13] P. J. French and A. G. R. Evans, "Polycrystalline silicon as a strain gauge material," *J. Phys. E: Sci. Instrum.*, vol. 19, p. 1055, 1986.
[14] M. W. Putty, S. C. Chang, R. T. Howe, A. L. Robinson and K. D. Wise, "One-port active polysilicon resonant microstructures," in *Proc. Micro Electro Mechanical Systems (MEMS '89)* (Salt Lake City), Feb. 20-22, 1989, pp. 60-65.

Albert Prak was born on October 4, 1964, in Holten, the Netherlands. He received his M.Sc. in 1989 from the University of Twente on the subject of damping behavior of micromechanical resonant diaphragms in air. Since 1989 he has been working towards his Ph.D., which is in the field of micromechanical resonant sensors, at the same university.

Miko Elwenspoek received his M.Sc. and Ph.D. from the Freie Universität Berlin, Germany, the latter on dynamical properties of liquid metals and alloys. From 1983 to 1987 he did research on the kinetics of crystal growth at the University of Nijmegen, The Netherlands.

Since 1987 he has been an Associate Professor in charge of the micromechanics group of the MESA Research Institute. Dr. Elwenspoek is a member of the MME (Micro Mechanics Europe) steering committee and of the MEMS steering committee.

Jan H. J. Fluitman (Member IEEE) was born on March 23, 1938, in Beverwijk, The Netherlands. He received his M.Sc. and Ph.D. degrees in physics from the University of Amsterdam in 1966 and 1970 respectively in the field of low-temperature solid-state physics. He joined the University of Twente in 1970. His research interest include magnetic recording, optical waveguide sensors, and micromechanics. Since 1982 he has been a full professor of transducer science and first chairman of the Sensors and Actuators Research Unit. Since 1990 he has also been Scientific Director of the MESA Research Institute, which combines microelectronics and S&A activities.

Dr. Fluitman is a member of the MEMS steering committee, the Eurosensors steering committee, and the World Micro Systems Technology Association.